

1 **Title:** Population turnover reverses classic island biogeography predictions in river-like  
2 landscapes

3 **Running Head:** Biodiversity in river-like landscapes.

4 **Authors:** Eric Harvey<sup>1,2\*</sup>, Isabelle Gounand<sup>1,2\*</sup>, Emanuel A. Fronhofer<sup>1,2</sup>, and Florian  
5 Altermatt<sup>1,2</sup>

6 \*These authors contributed equally to this work

7 **Corresponding Author:** [eric.harvey@eawag.ch](mailto:eric.harvey@eawag.ch)

8 **Affiliations:**

9 <sup>1</sup>Department of Evolutionary Biology and Environmental Studies, University of Zurich,  
10 Winterthurerstrasse 190, CH-8057 Zürich, Switzerland.

11 <sup>2</sup>Eawag, Swiss Federal Institute of Aquatic Science and Technology, Department of  
12 Aquatic Ecology, Überlandstrasse 133, CH-8600 Dübendorf, Switzerland

13 **Statement of authorship:** EH, IG, EAF and FA designed the research; IG and EAF  
14 designed the model; IG programmed and ran the model, analyzed the simulation data  
15 with support from EAF and produced the figures; EH conducted the lab experiment with  
16 support from IG, EAF and FA, processed the experimental data with support from IG,  
17 and carried out the analysis of experimental data; all authors participated in results  
18 interpretation; EH wrote the first draft of the manuscript; All authors significantly  
19 contributed to further manuscript revisions. EH and IG contributed equally to this work.

20 **Keywords:** Meta-community, Dendritic Networks, Biodiversity, Turnover, Patch size,  
21 Perturbations

## 22 **Background**

23 Motivated by the global biodiversity crisis, ecologists have spent the last decades  
24 identifying biodiversity hotspots. While these global analyses of biodiversity show  
25 recurrent patterns of spatial distributions worldwide, unveiling specific drivers remains  
26 logistically challenging. Here, we investigate the processes underlying biodiversity  
27 patterns in dendritic, river-like landscapes, iconic examples of highly diverse but  
28 threatened ecosystems. Combining theory and experiments, we show that the distribution  
29 of biodiversity in these landscapes fundamentally depends on how ecological selection is  
30 modulated across the landscape: while uniform ecological selection across the network  
31 leads to higher diversity in confluences, this pattern can be inverted due to patch size-  
32 dependent population turnover. Higher turnover in small headwater patches can slow  
33 down ecological selection, increasing local diversity in comparison to large confluences.  
34 Our results provide a way forward in the long-standing debate regarding the distribution  
35 of diversity in river-like landscapes within a single, experimentally validated conceptual  
36 framework.

37

38 Local species diversity in dendritic, river-like landscapes is generally expected to be  
39 higher in larger, more connected confluences than in headwaters<sup>1-5</sup>. Previous theoretical,  
40 comparative and experimental studies have all emphasized the importance of dispersal  
41 along the network structure of the landscape as a key driver of this diversity pattern,  
42 regardless of the specific dominant local drivers of community dynamics (such as  
43 ecological drift<sup>3,6</sup> or ecological selection<sup>7</sup>). The pattern of lower local diversity in  
44 upstream habitats compared to downstream confluences (hereafter ‘classical pattern’),  
45 however, is not ubiquitous in natural river systems: recent empirical studies<sup>8,9</sup> have  
46 documented that diversity patterns can be completely reversed, with higher diversity  
47 upstream rather than downstream (hereafter ‘reversed pattern’). These contrasting  
48 empirical patterns, especially the reversed one, and the transition from one to the other  
49 remain insufficiently understood and are currently not accounted for by any theoretical or  
50 experimental work. Given that river ecosystems support roughly 10% of all animal  
51 species on only 0.01% of the globe surface<sup>10</sup>, it is surprising and disturbing that we are  
52 still lacking a general understanding of the processes driving diversity patterns and the  
53 transition between seemingly opposed empirical patterns of diversity in these ecosystems.  
54 A better understanding of the dominant mechanisms generating contrasting diversity  
55 patterns is essential if we hope to counter current trends of erosion of biodiversity and  
56 ecosystem services in river ecosystems worldwide<sup>11-13</sup>.

57 River-like landscapes are structured by spatial flows of organisms and resources. They  
58 also inherently display strong environmental gradients, both in terms of resources (habitat  
59 size / land use influence) and perturbations (current flow, erosion)<sup>1,14</sup>. While previous  
60 theoretical work has primarily focused on dispersal-related mechanisms<sup>3,15,16</sup>, the latter

61 intrinsic characteristics might be key to explaining contrasting diversity patterns in such  
62 spatially structured landscapes where habitat size scales with position in the landscape<sup>4,17</sup>;  
63 While small headwater patches can be found across a wide range of landscape  
64 connectivity, the fewer and larger downstream patches are inherently more connected<sup>14</sup>.  
65 The Theory of Island Biogeography<sup>18,19</sup> ('TIB') provides explanation for one of the most  
66 established and universal ecological patterns stating that smaller and more isolated  
67 patches suffer higher extinction rates and lower immigration rates eventually leading to  
68 lower diversity than in larger and more connected patches<sup>18-22</sup>. In such a scenario,  
69 competitive exclusion due to ecological selection occurs more rapidly in small headwater  
70 communities because, in finite populations, extinction thresholds are reached earlier.  
71 Consequently, all else being equals, at equilibrium density, smaller patches should always  
72 contain lower diversity. In that context the 'reversed pattern' can only occur if (i) all else  
73 is not equal and smaller headwater patches contain higher environmental heterogeneity or  
74 (ii) equilibrium density is reached more slowly in smaller patches. The former represents  
75 the obvious case where headwater patches might contain higher proportion of micro-  
76 habitats providing higher niche dimensionality and/or *refugia* from competition and  
77 predation. Here we focus on the latter case, where perturbations maintain smaller patches  
78 away from their community equilibrium state. This is an especially likely and  
79 increasingly widespread scenario in the context of global change<sup>23</sup>. However, due to  
80 multiple interacting factors and lack of replication, it is highly challenging to be directly  
81 test in the field. To get a causal understanding, we thus develop first a general  
82 mathematical model, and then test the main predictions in well-established ecological  
83 microcosms.

84 Perturbations and associated increased population turnover are often seen as a major  
85 driver of community dynamics by slowing down competitive exclusion and ultimately  
86 favouring species coexistence<sup>24-26</sup>. If perturbations impact smaller patches more strongly  
87 than larger patches, it will generate higher population turnover in smaller patches that, in  
88 turn, can potentially lead to higher species richness in smaller headwater patches than in  
89 larger downstream patches. Thus, in the classical biodiversity pattern, competitive  
90 exclusion by ecological selection is expected to occur faster in smaller patches because of  
91 finite population sizes, while in the presence of perturbations higher population turnover  
92 in smaller patches should slow down competitive exclusion making selection slower in  
93 smaller patches thus potentially reversing biodiversity pattern in the landscape.

94 Indeed, beyond the structural properties of river-like landscapes, specific  
95 characteristics of headwaters also suggest that they are naturally more prone to  
96 perturbations<sup>27</sup> and thus to higher population turnover rates. For instance, headwaters  
97 exhibit higher benthic surface area to water volume ratio<sup>28</sup> and thus are more sensitive to  
98 minor changes to their surrounding environment<sup>29,30</sup>. Furthermore, they expand into  
99 higher elevations, which are experiencing harsher and more variable environmental  
100 conditions<sup>31</sup>. Eventually, this asymmetry in population turnover between upstream and  
101 downstream patches due to perturbations may generate higher diversity upstream  
102 compared to downstream patches.

103 To resolve the apparent inconsistency in our understanding of local diversity patterns  
104 in river-like landscapes<sup>3,8,9,16,32</sup>, we here investigate the processes underlying the  
105 distribution of biodiversity and specifically focus on characteristic patch size distributions  
106 and population turnover. In natural riverine landscapes, patch size distribution, network

107 configuration and perturbations are intrinsically linked, and cannot be disentangled in a  
108 causal approach (see also <sup>4,14,33</sup>). We thus used a general model reproducing river-like  
109 networks properties to disentangle spatial patterns of population turnover from other  
110 drivers of biodiversity. We then also validated the predicted turnover-induced reversed  
111 biodiversity pattern with a simple experiment. We first show theoretical results from a  
112 spatially explicit Lotka-Volterra competition metacommunity model. The model includes  
113 dispersal along dendritic networks, demographic stochasticity, and patch size-dependent  
114 turnover, that is, higher mortality in smaller patches (see full details in Methods). We  
115 secondly corroborated experimentally the model's main prediction on population  
116 turnover effects, using dendritic protist microcosm landscapes<sup>34</sup> of the same network  
117 topologies (see Methods and Fig. 1). Patch size-dependent turnover was experimentally  
118 reproduced by sampling, killing and pouring back (no change in biomass) a fixed volume  
119 of each community, which resulted in a gradient of population turnover from smaller  
120 upstream to larger downstream microcosms (13%, 8%, 4%, and 2% mortality). This  
121 mortality gradient implementing an inverse relationship between population turnover and  
122 patch size, can be seen as a general effect of environmental perturbation (perturbation-  
123 induced turnover).

124

## 125 **Results**

126 **Classical diversity pattern.** In the simulations without perturbation-induced population  
127 turnover, the highest diversity levels are found in the large downstream patches (Fig. 1  
128 and 2a). Contrastingly, the smaller, mostly upstream patches have lower diversity levels.

129 This differences in diversity unfolded with smaller patches supporting smaller population  
130 sizes (Fig. 3a), which are then more sensitive to stochastic extinctions relative to  
131 populations in larger patches (Fig. 3b).

132 **Reversed diversity pattern.** In the simulations with a gradient of perturbation-induced  
133 population turnover, highest diversity levels are found in upstream patches (Fig. 1 and  
134 2b) consistently across all the different community (different species traits) and landscape  
135 (different spatial networks) replicates. The same pattern was found in the context of our  
136 experiment with an aquatic protist community (Fig. 1 and 2c): As in the simulations  
137 (Supplementary Fig. 1), the biodiversity pattern appeared progressively over time with no  
138 apparent effects of patch size at the first sampling day (experiment day 7,  $7.4 \pm 0.67$   
139 species in smallest vs.  $7.1 \pm 0.70$  species in largest patches, mean  $\pm$  sd, Supplementary  
140 Fig. 2 and Table 1) compared to the final experimental day 29, when there was a clear  
141 and significant decline in local diversity with patch size ( $4.7 \pm 1.3$  species in smallest  
142 patches vs.  $2.5 \pm 1.5$  species in largest patches, mean  $\pm$  sd, Fig.1, 2b and Supplementary  
143 Table 1). The simulations show that, overall, patch size-dependent population turnover  
144 slows down ecological dynamics (ecological selection; Fig. 3a), but does more so in  
145 smaller patches (Fig. 3a), which is then increasing the time to extinction of less  
146 competitive species (Fig. 3b).

147 **Persistence of diversity patterns in river-like landscapes.** Our model predicts both  
148 diversity scenarios to occur within specific parts of the parameter space defined by the  
149 magnitude of dispersal and the strength of patch size-dependent population turnover (i.e.,  
150 slope of the relationship between patch size and population turnover rate, see Methods for  
151 details; Fig. 4): weak patch size-dependent population turnover generates the classical

152 diversity pattern, while intermediate to high strengths of patch size-dependent population  
153 turnover generate the reversed diversity pattern until population turnover is so high in  
154 smaller relative to larger patches that all species upstream go extinct, leading to a return  
155 to the classical diversity pattern. As expected, regardless of the strength of patch size-  
156 dependent population turnover, increasing dispersal blurs diversity patterns by  
157 homogenizing diversity in the landscape (Fig. 4).

158

## 159 **Discussion**

160 Testing the impact of perturbation-induced population turnover on the distribution of  
161 biodiversity in river-like landscapes, we found that turnover can alter the classical  
162 biodiversity pattern of higher diversity in larger downstream patches predicted by the  
163 TIB<sup>3,6,18</sup>: the classical pattern persists only until a certain level of population turnover, at  
164 which point asymmetry in turnover between smaller upstream and larger downstream  
165 patches will reverse the pattern completely. Such a reversed diversity pattern has been  
166 observed in case studies from multiple natural systems<sup>8,9</sup> and has challenged the idea of  
167 one overarching and universal diversity pattern to be expected in river-like landscapes (as  
168 proposed by some studies<sup>3,16,35,36</sup>). However, this reversal has hitherto neither been  
169 understood mechanistically nor predicted by current theory. Here, we provide a clear  
170 mechanistic explanation based on theoretical considerations, which we then successfully  
171 validated experimentally.

172 Dispersal and the landscape context are key factors in driving metacommunity  
173 dynamics<sup>37</sup>. Here we showed that specific characteristics of river-like landscapes, namely



174 a combination of the spatial distribution of patch sizes and an associated population  
175 turnover gradient, can also play a dominant role in driving diversity patterns. Higher  
176 population turnover in smaller headwater patches keeps communities away from their  
177 equilibrium state and thus reduces the strength of local ecological selection. This leads to  
178 the coexistence of more species for longer periods of time in comparison to larger  
179 patches, in which turnover is not strong enough to prevent competitive exclusion. This  
180 effect will be especially pronounced in communities with strong competitive asymmetries  
181 and even enhanced in systems with competition-colonization trade-offs, as few strong  
182 competitors with low dispersal rates, would lead to strong selection in the absence of  
183 turnover.

184 Our work suggests that there may be general mechanisms responsible for the naturally  
185 observed diversity patterns including the reversal of diversity patterns. Perturbation-  
186 mediated slowing down of competitive exclusion is a well-understood ecological  
187 mechanism affecting population dynamics<sup>25,38-40</sup>. Here we show that this mechanism can  
188 generate a specific signature in terms of biodiversity patterns when applied over a spatial  
189 gradient in perturbation, which are a common feature of river-like landscape. For  
190 instance, headwaters in river systems are naturally more prone to higher levels of  
191 population turnover because of their higher benthic surface area to water volume ratio  
192 compared to larger downstream patches<sup>28</sup>. Headwaters are also more exposed to changes  
193 in their surrounding environment, such as natural fire dynamics, potentially leading to  
194 more frequent flooding events, higher erosion levels and a decline in terrestrial subsidy  
195 (leaf input) on which they are energetically more dependent than larger downstream  
196 patches<sup>29,41</sup>. They are on average also located at higher elevation, and thus experiencing

197 stronger variations in temperature and weather conditions. Human-induced perturbations  
198 in pristine headwaters are increasingly common<sup>30</sup> and the general mechanisms  
199 demonstrated by our study suggest that these anthropogenic impacts can have unexpected  
200 large-scale consequences by inverting biodiversity patterns. This is especially true if  
201 perturbations occur in combination with invasive species, which is a common scenario<sup>42</sup>.  
202 Thereby, size-dependent population turnover leads to species-poor and highly invasion-  
203 prone communities at downstream sections of the river network, whereas species-rich  
204 upstream sections may be more resilient due to slower competitive exclusion In  
205 conclusion, we show that patch size-dependent turnover, which is intrinsic to river-like  
206 landscapes, and its effect on ecological selection can be a key mechanisms responsible  
207 for shaping the distribution of biodiversity distribution in river-like landscapes.

208

## 209 **Methods**

210 **Simulation experiment.** To investigate the mechanisms underlying biodiversity  
211 distribution in dendritic, river-like networks in relation to their intrinsic non-random  
212 patch connectivity/size pattern, we first used general simulations of a Lotka-Volterra  
213 competition model for 10 species, in which the temporal variation of species  $i$  density in  
214 patch  $x$ ,  $N_{ix}$  is described by:

$$215 \quad \frac{dN_{ix}}{dt} = r_i N_{ix} \left( 1 - \frac{\sum_{j=1}^n \alpha_{ij} N_{jx}}{K_i V_x} \right) - \frac{d}{V_x} \sum (N_{ix} - N_{iz}) - m_x N_{ix} + a * \rho \sqrt{N_{ix}}$$

216 where  $r_i$  is the intrinsic growth rate,  $\alpha_{ij}$  the per capita effect of species  $j$  on species  $i$   
217 (interaction coefficient),  $K_i$  the carrying capacity, which is scaled with the size of the

218 patch  $V_x$ ,  $d_i$  the dispersal rate and  $m_i$  the patch size-dependent mortality rate (population  
219 turnover). In the last term we model demographic stochasticity as in Giometto et al.<sup>43</sup>. At  
220 each time step, a proportion  $a$  times  $\rho$  of the square root of population density is being  
221 either added or removed from each species population in each patch; the parameter  $a$   
222 modulating the magnitude of this drift is set to 0.25 in all simulations; the random factor  
223  $\rho$  is sampled for each species within a patch at each time step from a Gaussian  
224 distribution of mean  $\mu = 0$  and variance  $\sigma = 0.1$ . Species traits were parameterized in a  
225 very simple and general way, independent of our experimental organisms, to preserve the  
226 generality of our model predictions. To limit sources of variations,  $r$ ,  $K$  and  $d$  are the  
227 same for all species in all patches and we implement species differences via interaction  
228 coefficients only. Interaction coefficients are drawn from a Gaussian distribution  
229 ( $\mu = 2$ ,  $\sigma = 0.25$ ) with all negative coefficients multiplied by -1 to obtain a purely  
230 competitive community;  $r$  and  $K$  were set to 0.25 and 2000 respectively in all  
231 simulations. The dispersal term is a sum function of the population density differences  
232 between patch  $x$  and each patch  $z$  to which it is connected according to the specific  
233 topology of the dendritic landscape. We scale dispersal rates with patch size to make it  
234 comparable to the experimental set-up where exchanging a constant volume between two  
235 patches was the most feasible dispersal mode. However, the results are robust to change  
236 in dispersal mode, using a constant rate either per vertex or per patch. As a minimal  
237 assumption to implement patch size dependency in turnover rates, we make mortality  
238 rates follow a linear relationship with patch size (see sensitivity analysis below for the  
239 values).

240 For the landscapes, we use river-like networks generated from five different space-  
241 filling optimal channel networks<sup>44</sup> known to reproduce the scaling properties observed in  
242 real river systems<sup>4,45</sup>. In order to also be able to use the same landscapes in the  
243 experiments, a coarse-graining procedure is used to reduce the 5 generated constructs to  
244 equivalent 6x6 patch networks, preserving the characteristics of the original three-  
245 dimensional basin (see Fig.1, for details see appendix A in Carrara et al.<sup>4</sup>), but having a  
246 total node size that was experimentally feasible. These 6x6 patch networks contained 36  
247 patches of four different volumes ( $V$ ) respecting river system scaling properties: 7.5, 13,  
248 22.5, and 45 mL (see Fig.1). These volume values are used for patch sizes  $V_x$  in the  
249 model.

250 Using these simulation settings, we test the effect of patch size-dependent population  
251 turnover on biodiversity patterns by contrasting simulations with and without turnover.  
252 We have two levels of replication: we replicate our simulations over the 5 different  
253 dendritic landscapes to assess the independence of the results from specific network  
254 topologies, and 10 random realisations of the interaction matrix (replicate communities),  
255 leading to 50 simulations total per scenario (turnover settings at a given dispersal rate).  
256 Simulations always start with all species already present in all patches and with same  
257 absolute density set to 200 individuals. The results are robust to starting conditions with  
258 same relative density (scaled to patch size). Simulations are run until 400 time steps,  
259 which is sufficient to observe competitive exclusion (see Fig. 3 and Supplements Figure 1  
260 for examples of dynamics). A species for which density falls below  $10^{-3}$  is considered  
261 extinct and its density set to 0. The results are robust to the decline or suppressing of this  
262 threshold but we keep it to optimize the computation time.

263 In addition, we explore the persistence of the different observed diversity patterns as a  
264 function of the magnitude of dispersal and the strength of the turnover vs. patch size  
265 relationship (slope of the relationship, see Fig. 4). We explore 6 levels of dispersal with  
266  $d \in \{0,0.05,0.1,0.25,0.5,1\}$  and 21 mortality rate combinations between the largest and  
267 the smallest patches, that is all combinations with  $m \in \{0,0.01,0.05,0.1,0.25,0.5\}$  with  
268 mortality in smallest patches being higher or equal to in largest patches (Supplementary  
269 figure 3). This results in 14 different slopes of the relationship between turnover  
270 (mortality rate) and patch size, ranging from 0 to  $-1.33$ . For each parameter combination  
271 we run 50 simulations (i.e., 5 replicate landscapes x 10 replicate communities) resulting  
272 in a total of 6,300 simulations.

273 **Experimental validation.** To empirically validate the main finding from our  
274 simulations, that is, patch size-dependent population turnover leading to a reversal of the  
275 ‘classical’ biodiversity pattern in dendritic network, we conducted a protist meta-  
276 community experiment. We did not experimentally test for the diversity pattern without  
277 perturbations because it has already been empirically verified many times in the  
278 literature<sup>2,3,7,27,46,47</sup>, and in the same experimental conditions<sup>4,16</sup>. Therefore, we focussed  
279 here on testing specific predictions from the simulations owing to patch-size dependent  
280 turnover and the occurrence of the predicted pattern of biodiversity under this scenario. In  
281 that context, the experiment constitutes a very conservative test of our much more general  
282 simulations. The experiment consisted of seven protist species interacting and dispersing  
283 for 29 days along 4 different dendritic networks of 36 patches (same than four of the five  
284 landscapes used in the simulations; see Fig. 1). Each landscape had 4 different patch size  
285 levels (7.5, 13, 22.5, and 45 mL) connected by dispersal along a dendritic network and

286 preserving the scaling properties observed in real river systems (see Fig. 1 and  
287 Supplementary figure 4 for a photo, and section “simulation experiment” above,  
288 following Carrara et al.<sup>4</sup>).

289 Our communities were composed of three bacteria species (*Serratia fonticola*, *Bacillus*  
290 *subtilis* and *Brevibacillus brevis*) fed upon by seven bacterivorous protist and one rotifer  
291 species (henceforth called “protists”): *Tetrahymena* sp., *Paramecium caudatum*,  
292 *Colpidium striatum*, *Spirostomum* sp., and *Chilomonas* sp., *Blepharisma* sp. and the  
293 rotifer *Cephalodella* sp. The latter two species can, next to feeding on bacteria, to a lesser  
294 degree also predate on smaller protists. Prior to the beginning of the experiment, each  
295 protist species was grown in monoculture in a solution of pre-autoclaved standard protist  
296 pellet medium (Carolina Biological Supply, Burlington NC, USA, 0.46 g protist pellets 1  
297 L<sup>-1</sup> tap water) and 10% bacteria inoculum, until they reached carrying capacity (for  
298 methodological details and protocols see Altermatt et al.<sup>34</sup>). Protist abundance and  
299 diversity were measured by video recording combined with a trained algorithm to  
300 differentiate each species based on their morphological traits (see below).

301 Each microcosm in our four landscapes consisted of a 50 mL polypropylene falcon  
302 tube (VWR, Dietikon, Switzerland). At day 0, we pipetted an equal mixture of each of  
303 the seven species into each microcosm to reach the corresponding volume (7.5, 13, 22.5  
304 or 45 mL). Thus, protist communities were added at 15% of their carrying capacity and  
305 were allowed to grow 24 hours before the first dispersal event. Dispersal and imposed  
306 population turnover (see below) occurred two times per week, while sampling of the  
307 communities for species count was done once a week (two dispersal events between each  
308 sampling with always at least 48 hours between the last dispersal/turnover event and

309 sampling). Sampling events and counting were done at day 0, 7, 15, 21, 29 of the  
310 experiment, while dispersal and turnover events occurred at day 1, 4, 8, 11, 16, 19, 22, 25  
311 of the experiment.

312 Dispersal was done by pipetting a fixed volume per vertex (1 mL) to each of the  
313 connected patches. Dispersal was bi-directional along each vertex (1 mL from a to b and  
314 1 mL from b to a), which ensured the maintenance of the same volume in each patch  
315 throughout the duration of the experiment. Other experiments in the same settings and  
316 simulations have shown that directional dispersal tends to strengthen meta-population and  
317 community patterns compared with bi-directional dispersal, but with no qualitative  
318 differences in the observed patterns<sup>4,16,48</sup>. Thus, doing dispersal in this way is  
319 conservative. For dispersal we used a mirror landscape (following methods developed in  
320 Carrara et al.<sup>16</sup>): first, 1 mL was sampled for each vertex connecting a microcosm in the  
321 real landscape and then pipetted to the recipient microcosm, but in the mirror landscape.  
322 Once this was done for all microcosms, the content of each mirror microcosm was poured  
323 to the same microcosm in the real landscape. It is noteworthy, however, that because we  
324 started our simulations and experiment with species already assembled (all species were  
325 present at start in all patches), we probably are underestimating the importance of  
326 dispersal dynamics in the process of early assembly<sup>49</sup>.

327 Patch size-dependent population turnover was experimentally reproduced by  
328 sampling, killing and pouring back (no change in biomass) a fixed volume of each  
329 community, which resulted in a gradient of turnover from smaller upstream to larger  
330 downstream microcosms (13%, 8%, 4%, and 2%), and can be seen as the most general  
331 type of disturbance. For each mortality event, 1 mL was sampled from each microcosm

332 and microwaved until boiling to turn all living cells into detritus<sup>50</sup>. After a 1-hour cooling  
333 period at ambient temperature (20 °C), the microwaved sampled had reached ambient  
334 temperature again and were poured back into the same microcosm.

335 At each measurement day, 0.4 mL was sampled from each microcosm for the protist  
336 density measurements. Protist density was measured by using a standardized video  
337 recording and analysis procedure<sup>51,52</sup> (for details see Supplementary appendix A). In  
338 short, a constant volume (34.4 µL) of each 0.4 mL sample was measured under a  
339 dissecting microscope connected to a camera for the recording of videos (5 s per video,  
340 see Supplementary appendix A for further details on this method). Then, using a  
341 customized version of the R-package *bemovi*<sup>52</sup>, we used an image processing software  
342 (ImageJ, National Institute of Health, USA) to extract the number of moving organisms  
343 per video frame along with a suite of different traits for each occurrence (e.g., speed,  
344 shape, size) that could then be used to filter out background movement noise (e.g.,  
345 particles from the medium) and to identify species in a mixture (see Supplementary  
346 appendix A).

347 **Statistical analysis.** To test for the effect of patch size on protist local diversity we  
348 used a two-way linear mixed effect model testing the interactive effects of patch size and  
349 continuous time on protist species richness. To control for temporal pseudo-replication,  
350 we added replicate and time as nested random factors. The model was fitted by  
351 maximizing the restricted log-likelihood (“REML”, see <sup>53</sup>). The linear mixed effect  
352 model was conducted using the R-package *NLME*<sup>53</sup>. The complete results can be found  
353 in Supplementary Table 1.

354



355        **Data availability.** The main data and r-script to reproduce the experimental results  
356 can be downloaded from Dryad (DOI:XX.XXXX/Dryad.XXXXXX).

357

358        **Acknowledgement**

359        We thank S. Gut, S. Flückiger and E. Keller for help during the laboratory work.

360        Funding is from the Swiss National Science Foundation Grant PP00P3\_150698

361

## 362 **References**

- 363 1. Vannote, R. L., Minshall, G. W., Cummins, K. W., Sedell, J. R. & Cushing, C. E.  
364 The River Continuum Concept. *Can. J. Fish. Aquat. Sci.* **37**, 130–137 (1980).
- 365 2. Ward, J. V., Tockner, K., Arscott, D. B. & Claret, C. Riverine landscape diversity.  
366 *Freshw. Biol.* **47**, 517–539 (2002).
- 367 3. Muneeppeerakul, R. *et al.* Neutral metacommunity models predict fish diversity  
368 patterns in Mississippi–Missouri basin. *Nature* **453**, 220–222 (2008).
- 369 4. Carrara, F. *et al.* Complex interaction of dendritic connectivity and hierarchical patch  
370 size on biodiversity in river-like landscapes. *Am. Nat.* **183**, 13–25 (2014).
- 371 5. Deiner, K., Fronhofer, E. A., Mächler, E., Walser, J.-C. & Altermatt, F.  
372 Environmental DNA reveals that rivers are conveyor belts of biodiversity  
373 information. *Nat. Commun.* **7**, 12544 (2016).
- 374 6. Economo, E. P. & Keitt, T. H. Network isolation and local diversity in neutral  
375 metacommunities. *Oikos* **119**, 1355–1363 (2010).
- 376 7. Seymour, M., Fronhofer, E. A. & Altermatt, F. Dendritic network structure and  
377 dispersal affect temporal dynamics of diversity and species persistence. *Oikos* **124**,  
378 908–916 (2015).
- 379 8. Besemer, K. *et al.* Headwaters are critical reservoirs of microbial diversity for fluvial  
380 networks. *Proc R Soc B* **280**, 20131760 (2013).
- 381 9. Ruiz-González, C., Niño-García, J. P. & del Giorgio, P. A. Terrestrial origin of  
382 bacterial communities in complex boreal freshwater networks. *Ecol. Lett.* **18**, 1198–  
383 1206 (2015).

- 384 10. Balian, E. V., Segers, H., Lévêque, C. & Martens, K. The Freshwater Animal  
385 Diversity Assessment: an overview of the results. *Hydrobiologia* **595**, 627–637  
386 (2008).
- 387 11. Tockner, K. & Stanford, J. A. Riverine flood plains: present state and future trends.  
388 *Environ. Conserv.* **29**, 308–330 (2002).
- 389 12. Dudgeon, D. *et al.* Freshwater biodiversity: importance, threats, status and  
390 conservation challenges. *Biol. Rev.* **81**, 163–182 (2006).
- 391 13. Vörösmarty, C. J. *et al.* Global threats to human water security and river biodiversity.  
392 *Nature* **467**, 555–561 (2010).
- 393 14. Rodríguez-Iturbe, I. & Rinaldo, A. *Fractal River Basins: Chance and Self-*  
394 *Organization.* (Cambridge University Press, 2001).
- 395 15. Mari, L., Casagrandi, R., Bertuzzo, E., Rinaldo, A. & Gatto, M. Metapopulation  
396 persistence and species spread in river networks. *Ecol. Lett.* **17**, 426–434 (2014).
- 397 16. Carrara, F., Altermatt, F., Rodriguez-Iturbe, I. & Rinaldo, A. Dendritic connectivity  
398 controls biodiversity patterns in experimental metacommunities. *Proc. Natl. Acad.*  
399 *Sci.* **109**, 5761–5766 (2012).
- 400 17. Leopold, L. B., Wolman, M. G. & Miller, J. P. *Fluvial Processes in Geomorphology.*  
401 (Dover Publications, 1995).
- 402 18. MacArthur, R. H. & Wilson, E. O. An equilibrium theory of insular zoogeography.  
403 *Evolution* **17**, 373 (1963).
- 404 19. MacArthur, R. H. & Wilson, E. O. *The Theory of Island Biogeography.* (Princeton  
405 University Press, 1967).

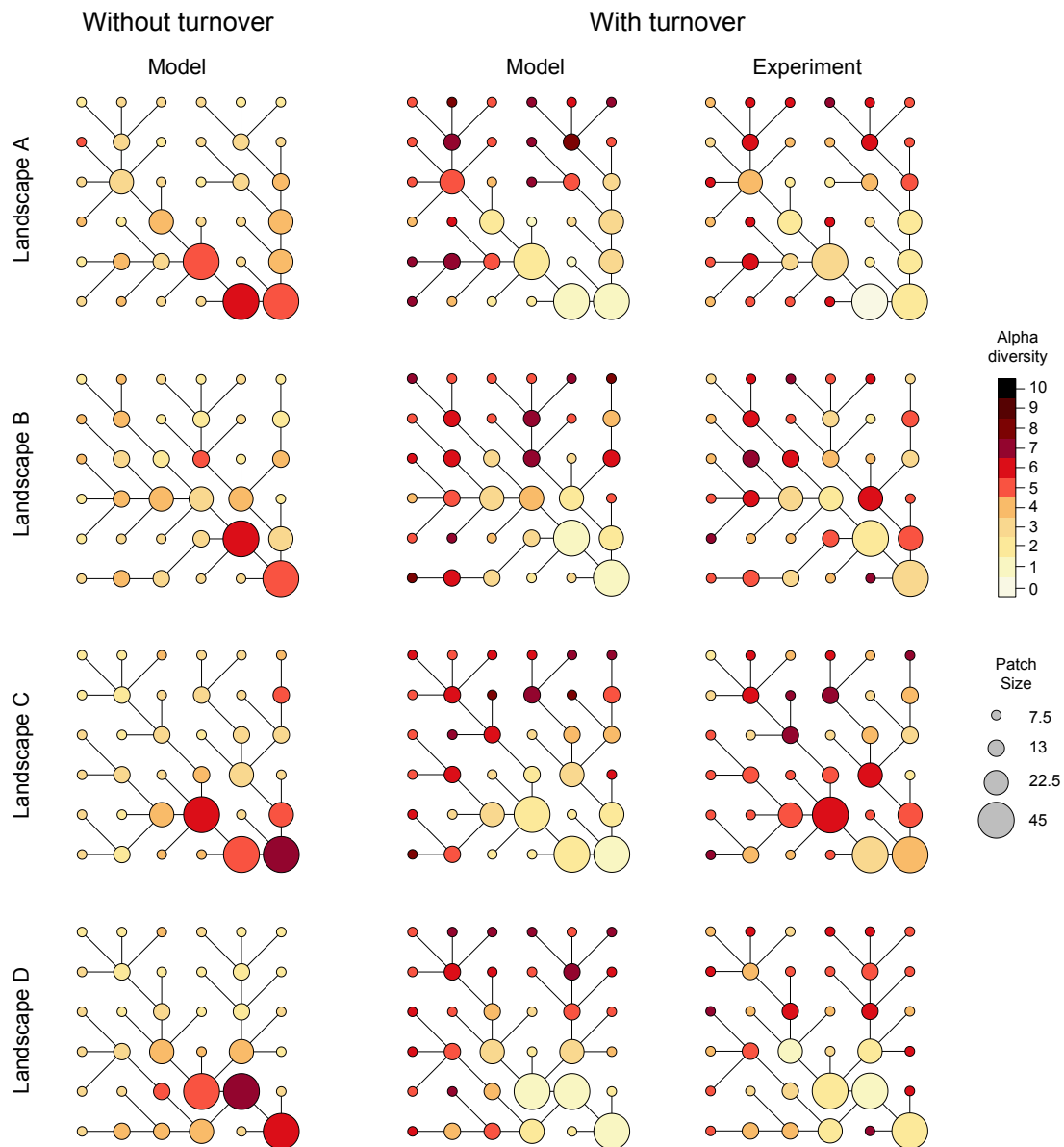
- 406 20. Hubbell, S. P. *The Unified Neutral Theory of Biodiversity and Biogeography*.  
407 (Princeton University Press, 2001).
- 408 21. Angela, D. Y. & Lei, S. A. Equilibrium Theory of Island Biogeography: A Review.  
409 *Proc. RMRS* 163 (1998).
- 410 22. Harvey, E. & MacDougall, A. S. Trophic island biogeography drives spatial  
411 divergence of community establishment. *Ecology* **95**, 2870–2878 (2014).
- 412 23. Ceballos, G. *et al.* Accelerated modern human-induced species losses: Entering the  
413 sixth mass extinction. *Sci. Adv.* **1**, e1400253 (2015).
- 414 24. Valladares, F., Bastias, C. C., Godoy, O., Granda, E. & Escudero, A. Species  
415 coexistence in a changing world. *Front. Plant Sci.* **6**, (2015).
- 416 25. Chesson, P. L. & Warner, R. R. Environmental variability promotes coexistence in  
417 lottery competitive systems. *Am. Nat.* **117**, 923–943 (1981).
- 418 26. Hutchinson, G. The paradox of the plankton. *Am. Nat.* **95**, 137–145 (1961).
- 419 27. Finn, D. S., Bonada, N., Múrria, C. & Hughes, J. M. Small but mighty: headwaters  
420 are vital to stream network biodiversity at two levels of organization. *J. North Am.*  
421 *Benthol. Soc.* **30**, 963–980 (2011).
- 422 28. Battin, T. J. *et al.* Biophysical controls on organic carbon fluxes in fluvial networks.  
423 *Nat. Geosci.* **1**, 95–100 (2008).
- 424 29. England, L. E. & Rosemond, A. D. Small reductions in forest cover weaken  
425 terrestrial-aquatic linkages in headwater streams. *Freshw. Biol.* **49**, 721–734 (2004).
- 426 30. Palmer, M. A. *et al.* Mountaintop mining consequences. *Science* **327**, 148–149  
427 (2010).

- 428 31. Clarke, A., Mac Nally, R., Bond, N. & Lake, P. S. Macroinvertebrate diversity in  
429 headwater streams: a review. *Freshw. Biol.* **53**, 1707–1721 (2008).
- 430 32. Altermatt, F. Diversity in riverine metacommunities: a network perspective. *Aquat.*  
431 *Ecol.* **47**, 365–377 (2013).
- 432 33. Thorp, J. H., Thoms, M. C. & Delong, M. D. The riverine ecosystem synthesis:  
433 biocomplexity in river networks across space and time. *River Res. Appl.* **22**, 123–147  
434 (2006).
- 435 34. Altermatt, F. *et al.* Big answers from small worlds: a user’s guide for protist  
436 microcosms as a model system in ecology and evolution. *Methods Ecol. Evol.* **6**,  
437 218–231 (2015).
- 438 35. Widder, S. *et al.* Fluvial network organization imprints on microbial co-occurrence  
439 networks. *Proc. Natl. Acad. Sci.* **111**, 12799–12804 (2014).
- 440 36. Bertuzzo, E., Maritan, A., Gatto, M., Rodriguez-Iturbe, I. & Rinaldo, A. River  
441 networks and ecological corridors: Reactive transport on fractals, migration fronts,  
442 hydrochory. *Water Resour. Res.* **43**, W04419 (2007).
- 443 37. Leibold, M. A. *et al.* The metacommunity concept: a framework for multi-scale  
444 community ecology. *Ecol. Lett.* **7**, 601–613 (2004).
- 445 38. Sheil, D. Disturbance and distributions: avoiding exclusion in a warming world. *Ecol.*  
446 *Soc.* **21**, (2016).
- 447 39. Chesson, P. Mechanisms of maintenance of species diversity. *Annu. Rev. Ecol. Syst.*  
448 **31**, 343–366 (2000).
- 449 40. Göthlich, L. & Oschlies, A. Disturbance characteristics determine the timescale of  
450 competitive exclusion in a phytoplankton model. *Ecol. Model.* **296**, 126–135 (2015).

- 451 41. Lowe, W. H., Likens, G. E. & Power, M. E. Linking scales in stream ecology.  
452 *BioScience* **56**, 591 (2006).
- 453 42. Seebens, H. *et al.* No saturation in the accumulation of alien species worldwide. *Nat.*  
454 *Commun.* **8**, 14435 (2017).
- 455 43. Giometto, A., Rinaldo, A., Carrara, F. & Altermatt, F. Emerging predictable features  
456 of replicated biological invasion fronts. *Proc. Natl. Acad. Sci.* 201321167 (2013).  
457 doi:10.1073/pnas.1321167110
- 458 44. Rigon, R., Rinaldo, A., Rodriguez-Iturbe, I., Bras, R. L. & Ijjasz-Vasquez, E.  
459 Optimal channel networks: A framework for the study of river basin morphology.  
460 *Water Resour. Res.* **29**, 1635–1646 (1993).
- 461 45. Rinaldo, A., Banavar, J. R. & Maritan, A. Trees, networks, and hydrology. *Water*  
462 *Resour. Res.* **42**, W06D07 (2006).
- 463 46. Altermatt, F., Seymour, M. & Martinez, N. River network properties shape  $\alpha$ -  
464 diversity and community similarity patterns of aquatic insect communities across  
465 major drainage basins. *J. Biogeogr.* **40**, 2249–2260 (2013).
- 466 47. Altermatt, F. *et al.* Diversity and distribution of freshwater amphipod species in  
467 Switzerland (Crustacea: Amphipoda). *PLoS ONE* **9**, e110328 (2014).
- 468 48. Fronhofer, E. A. & Altermatt, F. Classical metapopulation dynamics and eco-  
469 evolutionary feedbacks in dendritic networks. *Ecography* n/a-n/a (2017).  
470 doi:10.1111/ecog.02761
- 471 49. Walker, L. R. & Chapin, F. S. Interactions among Processes Controlling Successional  
472 Change. *Oikos* **50**, 131–135 (1987).

- 473 50. Harvey, E., Gounand, I., Ganesanandamoorthy, P. & Altermatt, F. Spatially  
474 cascading effect of perturbations in experimental meta-ecosystems. *Proc R Soc B*  
475 **283**, 20161496 (2016).
- 476 51. Pennekamp, F. & Schtickzelle, N. Implementing image analysis in laboratory-based  
477 experimental systems for ecology and evolution: a hands-on guide. *Methods Ecol.*  
478 *Evol.* **4**, 483–492 (2013).
- 479 52. Pennekamp, F., Schtickzelle, N. & Petchey, O. L. BEMOVI, software for extracting  
480 behavior and morphology from videos, illustrated with analyses of microbes. *Ecol.*  
481 *Evol.* **5**, 2584–2595 (2015).
- 482 53. Pinheiro, J., Bates, D., DebRoy, S., Sarkar, D. & R Core Team. *nlme: Linear and*  
483 *Nonlinear Mixed Effects Model.* (2016).
- 484
- 485
- 486
- 487
- 488

489 Figures



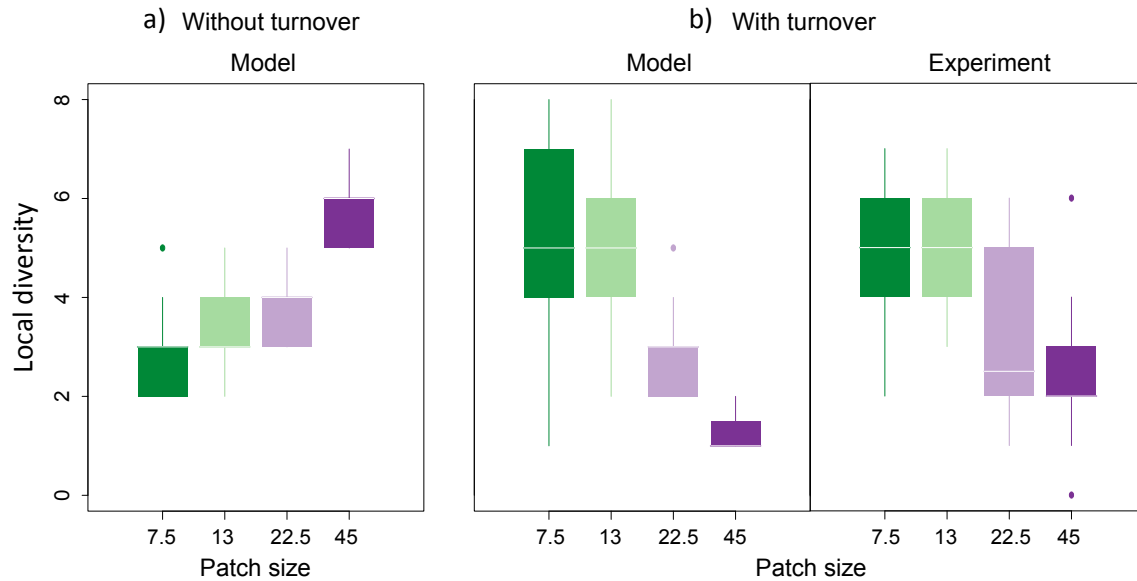
490

491 Figure 1. Diversity distribution (local species richness) in dendritic, river-like landscapes  
492 with and without patch size-dependent population turnover. The 'Model' landscapes  
493 displayed in this figure are example of simulations made with the same replicate  
494 community. Results were qualitatively similar for each of the 10 replicate communities  
495 randomly generated (see Supplementary Figure 1 for results with the different  
496 communities; the community used in the present figure is community 7); model  
497 parameters specific to these simulations are  $d = 0.05$ , patch size-dependent mortality  
498 rates  $m$  are 0.1, 0.0864, 0.064 and 0.01 respectively from smaller to larger patches. For



499 network graphs based on experimental results, each graph represents local diversity  
500 pattern for one of the four landscape replicates (A, B, C, and D). For illustration purpose,  
501 all network graphs are depicted at snapshots of diversity patterns at time steps of  
502 comparable local diversity: time steps 118.4 (simulations without population turnover;  
503 faster dynamics), 168.1 (simulations with population turnover; slower dynamics), and at  
504 experimental day 29 (last sampling day). See complete dynamics over time for model  
505 simulations on Supplementary figure 1 and for experimental results on Supplementary  
506 figure 2.

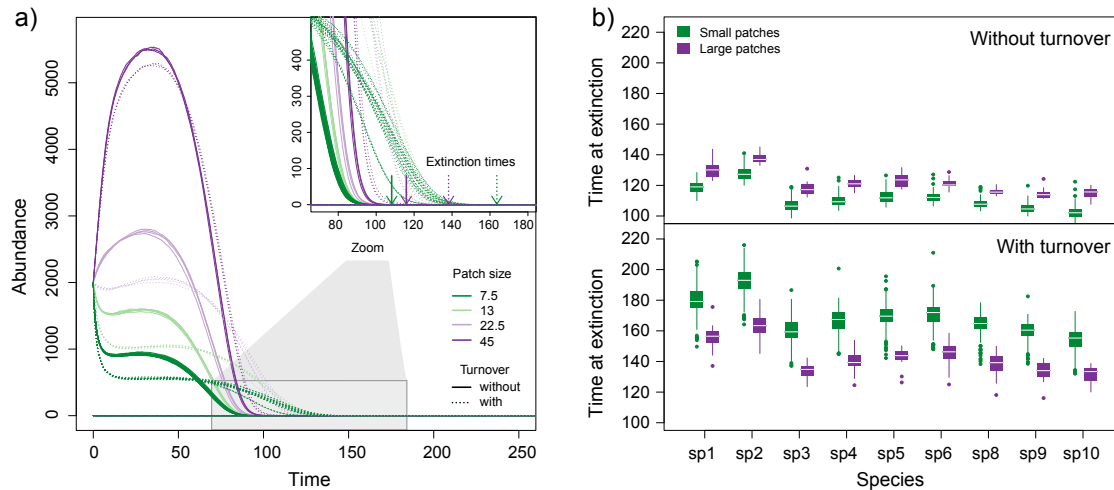
507



508

509 Figure 2. Diversity distribution in dendritic, river-like landscapes a) without and b) with  
510 patch size- dependent population turnover. For the panels based on simulations, each  
511 boxplot represents the distribution of diversity values across the 4 replicate landscapes  
512 used in the experiment, and for one of the 10 replicate communities that were used in the  
513 simulations (community 7 in Supplementary figure 1). Parameters and data are the same  
514 as in Figure 1. The two largest patch sizes of 45 (N=11) and 22.5 mL (N=14) show  
515 significant decline in local diversity compared to the smaller patch sizes of 13 (N=34)  
516 and 7.5 mL (N=85) (see Supplementary Table 1 for complete linear mixed effect model  
517 results).

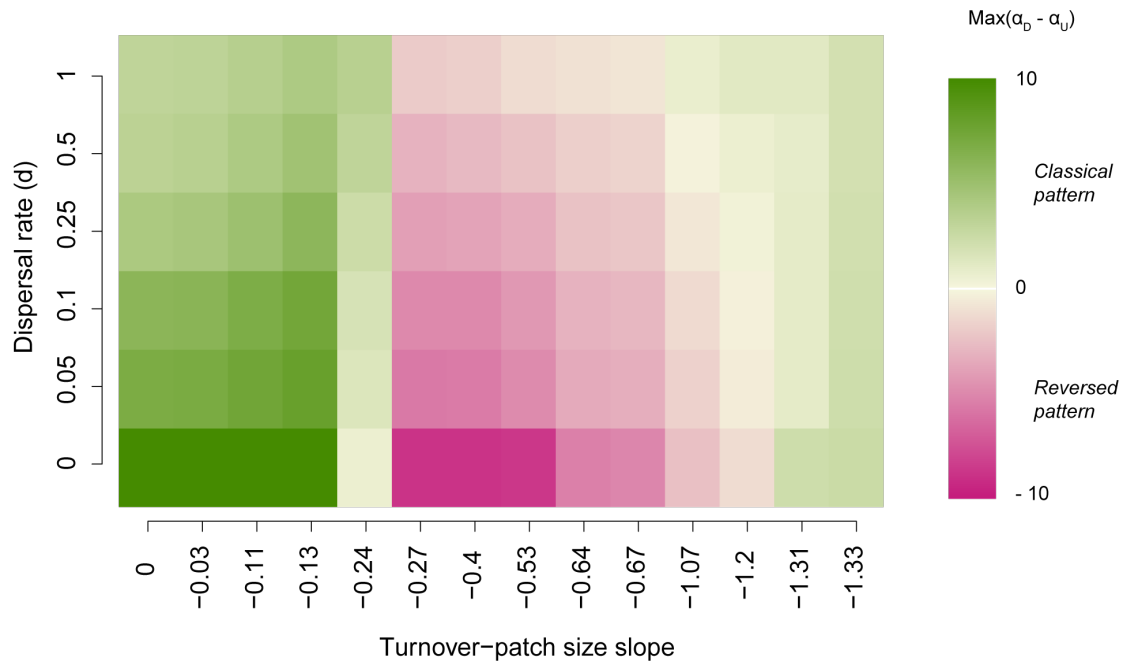
518



519

520 Figure 3. Time to extinction as a function of patch size-dependent turnover in the  
521 simulations. a) Temporal dynamics of one species with and without turnover (dotted and  
522 full lines respectively). Arrows indicate time at extinction for the smallest (green) and  
523 largest (purple) patches with and without turnover. b) Time at extinction for each species  
524 in the smallest and the largest patches with turnover (lower panel) or without turnover  
525 (upper panel). Each boxplot represents the distribution of values across the 4 replicate  
526 landscapes, and for one of the 10 different replicate communities that were used in the  
527 simulations (community 7 in Supplementary figure 1). Data and parameters are the same  
528 as in Figure 1. Temporal dynamics in a) are the ones of species 10 in community 7 in  
529 replicate landscape A.

530



531

532 Figure 4. Persistence of diversity patterns in dendritic, river-like landscapes. The figure  
533 illustrates the parameter space within which each diversity pattern is found as a function  
534 of the strength of patch size-dependent population turnover and the magnitude of  
535 dispersal (for all mortality combinations see Supplementary figure 3).  $\alpha_D - \alpha_U$  corresponds  
536 to the maximum observed difference, along the temporal dynamics, in richness between  
537 largest and smallest patches. When  $\alpha_D - \alpha_U$  is positive (green colours) the classical pattern  
538 emerges over the course of the dynamics, with higher diversity in large than in small  
539 patches, while when the difference is negative (pink colours) it is the reversed pattern,  
540 with higher diversity in small (i.e., headwater) rather than in large patches.

541